

# Development of Density and Temperature Boundary Condition Models in *L*-mode Tokamak Plasmas

**A. Siriwitpreecha**

Department of Industrial Physics and Medical Instrumentation, Faculty of Applied Science,  
King Mongkut's University of Technology North Bangkok, Bangkok, Thailand

**T. Onjun**

School of Manufacturing Systems and Mechanical Engineering, Sirindhorn International  
Institute of Technology, Thammasat University, Pathum Thani, Thailand

## Abstract

Models for predicting temperature and density at the edge of Low Confinement mode (*L*-mode) plasmas are developed. It is assumed in this work that the temperature and density at boundary of *L*-mode plasma are functions of plasma engineering controlled parameters, including plasma current, toroidal magnetic field, total heating power, line averaged density, hydrogenic mass, major radius, minor radius, inverse aspect ratio and elongation. A multiple regression technique is used to analyze 86 experimental data points of *L*-mode from AUG and JT60U tokamaks obtained from the latest public version of the International Pedestal Database (version 3.2). The RMSEs of temperature and density boundary models are found to be 24.41% and 14.27%, respectively. Self-consistent simulations of *L*-mode plasmas in DIII-D and TFTR tokamaks are carried out using BALDUR 1.5D integrated predictive modeling code. The combination of anomalous Multi-Mode (MMM95) and Mixed Bohm/gyro-Bohm (Mixed B/gB) transport models, together with the developed boundary models, are used to simulate the time evolution of temperature and density profiles for 13 *L*-mode discharges from DIII-D and TFTR tokamaks, including systematic scans over gyro-radius, plasma power, plasma current and plasma density. Statistical analysis is carried out to evaluate the agreement. For example, it is found that the average relative root mean square (RMS) deviation for each model and each kind of profile is less than the scatter within each transport model from one discharge to another. The RMS deviation of all discharges from either using MMM95 model or using Mixed B/gB model for the electron density profile varies from 2.00% to 16.41%, while the electron temperature profile varies from 3.34% to 27.94%, and the ion temperature profile varies from 4.17% to 38.87%. It is shown that the simulations using the MMM95 model tend to agree better with experimental data than those using the Mixed B/gB model, especially the ion and electron temperature profiles. In addition, these boundary conditions are used to simulate the plasma profiles in *L*-mode of ITER. It is found that the plasma performance in ITER is predicted to be in the range of Fusion Q and is approximately 4 for the *L*-mode condition (4.12 for MMM95 model and 3.59 for Mixed B/gB model).

**Keywords:** Simulation; *L*-mode; Edge density; Edge temperature; BALDUR

## 1. Introduction

The concept of magnetic confinement fusion has long been explored to address the feasibility of nuclear fusion energy. Burning plasma experiments, such as the International Thermonuclear Experimental Reactor (ITER), have been proposed to explore this possibility. The plasma in the Low Confinement mode (*L*-mode) regime is an interesting scenario for burning plasma experiments, due to high plasma stability and the simplicity in operation. However, the performance of *L*-mode plasmas is currently poorer than that of High Confinement mode (*H*-mode), Ref[1]. If the understanding of *L*-mode plasma is better, it could potentially improve the *L*-mode performance to be in a more desirable regime. One key understanding is the boundary conditions for both temperature and density. As a result, it is important to develop *L*-mode boundary models.

In previous study by G. Bateman *et al.*[3], BALDUR integrated predictive modeling code together with the Multimode (MMM95) core transport model was used to predict temperature and density profiles. It was found that those predicted profiles agreed with experimental data with an RMS deviation less than 15% for 41 *L*-mode and *H*-mode discharges from the TFTR(13), DIII-D(14) and JET(15). In Ref[4], the Mixed B/gB model and the MMM95 model were used to predict the plasma profiles such as electron density, ion and electron temperature in 13 discharges *L*-mode from DIII-D (4) and TFTR (9) tokamaks. In that work, the simulation profiles were compared with experimental data. Statistical analysis shows that simulation profiles from both transport models match experimental data equally well. The RMS deviation for electron density is less than 24.3%, while electron and ion temperature are less than 27.4% and 22.5%, respectively. It is worth mentioning that in both previous studies, the boundary con-

ditions were taken from experimental data. Linda E. Sugiyama [10] used the experimental *L*-mode database from 7 tokamaks for about 1088 discharges, Alcator C-Mod(348), DIII-D(72), FTU(138), JET(104), JT60(349), PDX(32) and TFTR(45) to fit the ITER 1996 *L*-mode power law scaling. The statistical power law regression fit all discharges, and the result of RMSE for this model is 23.6%. R. Hiwatari *et al.*[11] studied the confinement characteristics of dimensionally similar discharges in JT-60U *L*-mode plasma. The transport simulations were carried out with three different transport models, the Bohm type, the Current Diffusive Ballooning Mode, and the Multi Mode models. For all models, the electron stored energy is in agreement with experimental data within less than 15% and the standard deviation of the electron temperature profiles between experimental data and simulation results has at most 20%-30% difference. K.S. Riedel [12] found a scaling similar to Goldston scaling for the NB limiter dataset which and a scaling similar to ITER89P for the combined dataset, which consists of ISX-B, ASDEX, DIII, PDX, JET, JT-60 and TFTR tokamaks. This analysis was based on 705 data point subset of ITER *L*-mode database. The predicted ITER confinement time was 2.27 sec.

In this work, boundary condition models in *L*-mode plasmas, such as temperature and density models, are developed and compared with the experimental data obtained from AUG and JT60U tokamaks. The combination of anomalous transport models of either the MMM95 model or the Mixed-B/gB model, together with the developed boundary models, are used to simulate the time evolution of temperature and density profiles for 13 *L*-mode discharges from DIII-D and TFTR tokamaks. These simulation results will be compared to the experimental data for each discharge. The statistical analysis is used to quantify the comparison between the simulations and the experiments. In addition, these developed

models will be used to simulate the  $L$ -mode scenario of ITER.

This paper is organized as follows: brief descriptions of relevant components of the BALDUR code, including the MMM95 model and the Mixed B/gB model are presented in section 3; the development of boundary models for both temperature and density are described in section 2; a sensitivity study is described in section 4; and the conclusion is given in section 5.

## 2. Development of Boundary Models

The models for predicting temperature and density in  $L$ -mode tokamak plasma are developed using the experimental data obtained from the latest public version of the International Pedestal Database (version 3.2). It is assumed that the temperature and density scaling are found using the power scaling law which can be expressed in engineering parameters such as temperature, plasma current, toroidal magnetic field, total heating power, line averaged density, hydrogenic mass, major radius, minor radius, inverse aspect ratio and elongation at the separatrix. The notation of these parameters used in this paper is shown in Table 1.

**Table 1** Notation used in this paper

Symbol	Unit	Description
$T$	keV	temperature
$I_p$	MA	plasma current
$B_T$	T	toroidal magnetic field
$P_{heat}$	MW	total heating power
$n_{l,20}$	$\times 10^{20} \text{ m}^{-3}$	line averaged density
$A_H$		hydrogenic mass
$R$	amu	major radius
$a$	m	minor radius
$\varepsilon$	m	inverse aspect ratio
$\kappa$	-	plasma elongation
$t_{diag}$	s	diagnostic time

The prediction of temperature in  $L$ -mode tokamak plasma from empirical model using the power scaling law for temperature can be expressed as:

$$T_{bound} \propto I_p^a B_T^b P_{heat}^c n_{l,20}^d A_H^e R^f \varepsilon^g \kappa^h \quad (1)$$

and the power scaling law for density in  $L$ -mode tokamak plasma can be expressed as:

$$n_{bound} \propto I_p^a B_T^b P_{heat}^c n_{l,20}^d A_H^e R^f \varepsilon^g \kappa^h \quad (2)$$

where  $a, b, c, d, e, f, g, h$  are the constants, which can be found by fitting experimental data of engineering parameters in  $L$ -mode from database using statistical multiple regression analysis.

These models are carried out with the engineering parameters with 86 data points in  $L$ -mode from AUG(61) and JT60U(25). The predicted results of the temperature and density in  $L$ -mode tokamak plasma from empirical models using the power scaling law for temperature [keV] and density [ $\times 10^{20} \text{ m}^{-3}$ ] at the boundary can be expressed as:

$$T_{bound} = 13.60 I_p^{0.83} B_T^{0.11} P_{heat}^{0.54} A_H^{0.90} n_{l,20}^{-1.29} R^{-0.34} \varepsilon^{1.90} \kappa^{6.74} \quad (3)$$

$$n_{bound} = 0.31 I_p^{0.15} B_T^{-0.11} P_{heat}^{0.08} A_H^{0.07} n_{l,20}^{0.99} R^{-0.43} \varepsilon^{-0.66} \kappa^{0.26} \quad (4)$$

The empirical model for temperature at boundary is plotted against the experimental data and is shown in Fig.1. For the density model, Fig.2 shows the relation between the ratio of empirical density and experimental data to the Greenwald density ( $n_{gr} = I/\pi a^2$ ), the ratio of plasma current, and poloidal area of plasma.

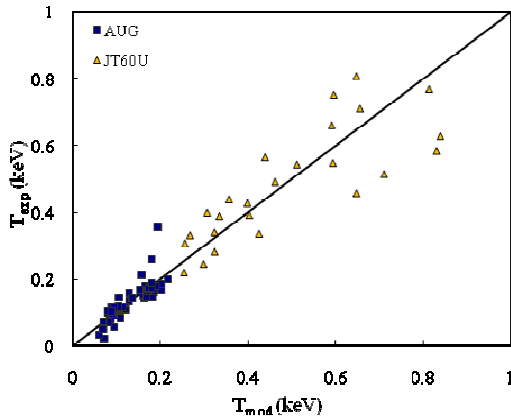


**Fig.1** The empirical model for temperature is plotted against experimental data.

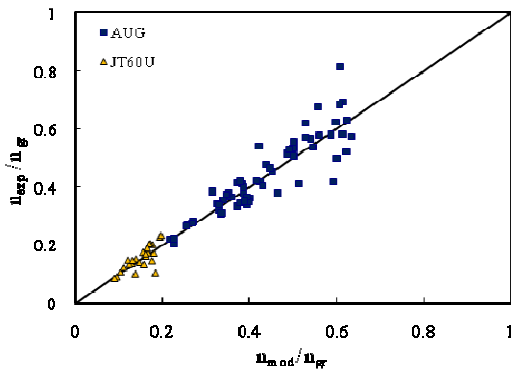


**Fig.2** The ratio of the density from the empirical model to the Greenwald density, is plotted against the ratio of experimental data to the Greenwald density.

It is found that the root mean square errors (RMSEs) of the scaling law for temperature [keV] and density [ $\times 10^{20}$  particles/m<sup>3</sup>] are 24.41% and 18.81%, respectively.

### 3. BALDUR Code

The BALDUR integrated predictive modeling code [6] is used to compute the time evolution of plasma profiles including electron and ion temperatures, deuterium and tritium densities, helium and impurity densities, magnetic  $q$ , neutrals, and fast ions. These time-evolving profiles are com-

puted in the BALDUR integrated predictive modeling code by combining the effects of many physical processes self-consistently, including the effects of transport, plasma heating, particle influx, boundary conditions, the plasma equilibrium shape, and sawtooth oscillations. Fusion heating and helium ash accumulation are computed self-consistently. The BALDUR simulations have been intensively compared against various plasma experiments, which yield an overall agreement of 10% RMS deviation [7, 8]. In BALDUR code, fusion heating power is determined using the nuclear reaction rates and a Fokker Planck package to compute the slowing down spectrum of fast alpha particles on each flux surface in the plasma [6]. The fusion heating component of the BALDUR code also computes the rate of production of thermal helium ions and the rate of depletion of deuterium and tritium ions within the plasma core. The brief details of these transport models are described below.

#### 3.1 The Mixed B/gB core transport model

The Mixed B/gB core transport model [9] is an empirical transport model. It was originally a local transport model with Bohm scaling. A transport model is said to be “local” when the transport fluxes (such as heat and particle fluxes) depend entirely on local plasma properties (such as temperatures, densities, and their gradients). A transport model is said to have “Bohm” scaling when the transport diffusivities are proportional to the gyro-radius times thermal velocity over a plasma linear dimension such as major radius. Transport diffusivities in models with Bohm scaling are also functions of the profile shapes (characterized by normalized gradients) and other plasma parameters such as magnetic  $q$  and minor radius. These parameters are all assumed to be held fixed in systematic scans in which only the gyro-radius is changed relative to plasma dimensions. The original JET model was subsequently

extended to describe ion transport, and a gyro-Bohm term was added in order for simulations to be able to match data from smaller tokamaks as well as data from larger machines. A transport model is said to have “gyro-Bohm” scaling when the transport diffusivities are proportional to the square of the gyroradius times thermal velocity over the square of the plasma linear dimension. The Bohm contribution to the JET model usually dominates over most of the radial extent of the plasma. The gyro-Bohm contribution usually makes its largest contribution in the deep core of the plasma and plays a significant role only in smaller tokamaks with relatively low power and low magnetic field [9].

### 3.2 The Multimode core transport model

The MMM95 model [3] is a linear combination of theory-based transport models which consists of the Weiland model for the ion temperature gradient (ITG) and trapped electron modes (TEM), the Guzdar–Drake model for drift-resistive ballooning modes, as well as a smaller contribution from kinetic ballooning modes. The Weiland model for drift modes such as ITG and TEM modes usually provides the largest contribution to the MMM95 transport model in most of the plasma core. The Weiland model is derived by linearizing the fluid equations, with magnetic drifts for each plasma species. Eigen values and eigenvectors computed from these fluid equations are then used to compute a quasilinear approximation for the thermal and particle transport fluxes. The Weiland model includes many different physical phenomena such as effects of trapped electrons,  $T_i \neq T_e$ , impurities, fast ions, and finite  $b$ . The resistive ballooning model in MMM95 transport model is based on the 1993 **ExB** drift-resistive ballooning mode model by Guzdar–Drake, in which the transport is proportional to the pressure gradient and collisionality. The contribution from the resistive ballooning model usually

dominates the transport near the plasma edge. Finally, the kinetic ballooning model is a semi-empirical model, which usually provides a small contribution to the total diffusivity throughout the plasma, except near the magnetic axis. This model is an approximation to the first ballooning mode stability limit. All the anomalous transport contributions to the MMM95 transport model are multiplied by  $4-\kappa$ , since the models were originally derived for circular plasmas.

## 4. Simulation results

In this work, the BALDUR integrated predictive modeling code is used to simulate the boundary profiles in  $L$ -mode scenario, which is from 13 discharges from TFTR and DIII-D tokamaks. The engineering parameter scans of all discharges are listed in Tables 2-4.

**Table 2** List of TFTR discharges in the engineering parameter scans

Tokamak Shot No.	TFTR 45359 low P	TFTR 45585 high P	TFTR 45966 low $I_p$	TFTR 45980 high $I_p$	TFTR 50921 low $\rho^*$
<i>R</i>	2.58	2.58	2.46	2.46	2.45
<i>A</i>	0.93	0.93	0.80	0.80	0.80
$\kappa$	1.00	1.00	1.00	1.00	1.00
$B_T$	3.75	3.75	4.76	4.76	2.14
$I_p$	1.79	1.79	1.00	2.00	0.89
$n_e$	4.65	3.23	3.31	3.57	1.77
$P_{aux}$	4.52	19.20	11.40	11.30	4.66
$t_{diag}$	4.41	4.17	4.90	3.47	3.95

**Table 3** List of TFTR discharges in the engineering parameter scans (continue)

Tokamak Shot No.	TFTR 50904 med $\rho^*$	TFTR 50911 high $\rho^*$	TFTR 62270 low $n_e$	TFTR 62248 high $n_e$
<i>R</i>	2.45	2.45	2.45	2.45
<i>a</i>	0.80	0.80	0.80	0.80
$\kappa$	1.00	1.00	1.00	1.00
$B_T$	2.86	4.26	4.75	4.77
$I_p$	1.19	1.78	1.78	1.78
$n_e$	2.58	4.46	3.59	5.30
$P_{aux}$	7.17	17.66	7.43	14.8
$t_{diag}$	3.95	3.93	4.03	4.03

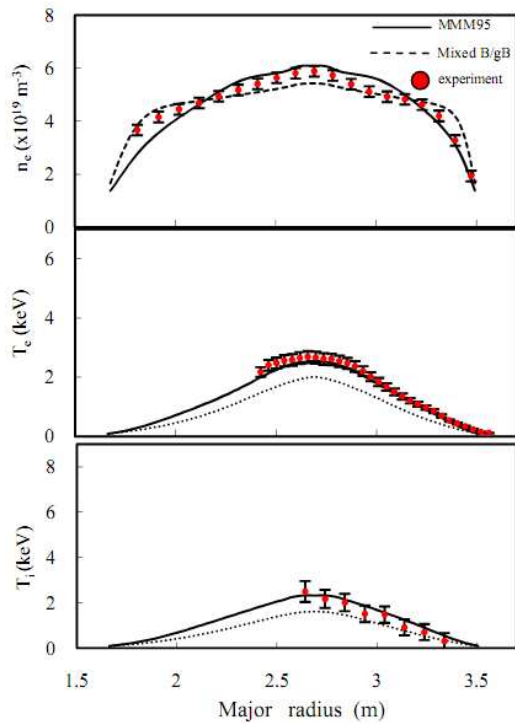
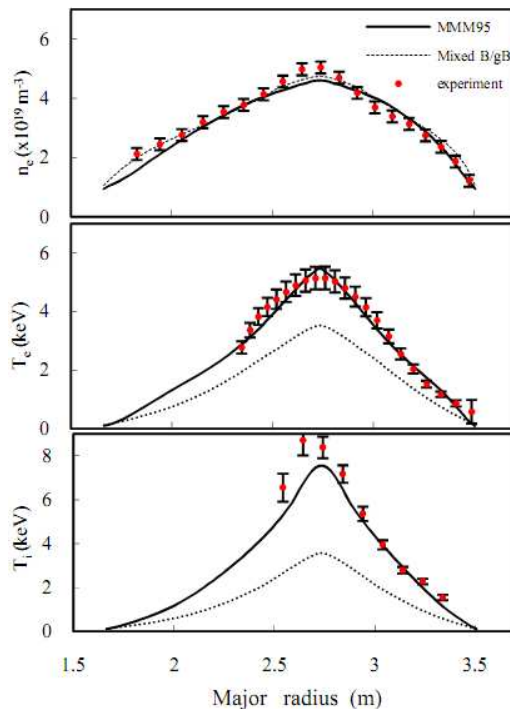
**Table 4** List of DIII-D discharges in the engineering parameter scans

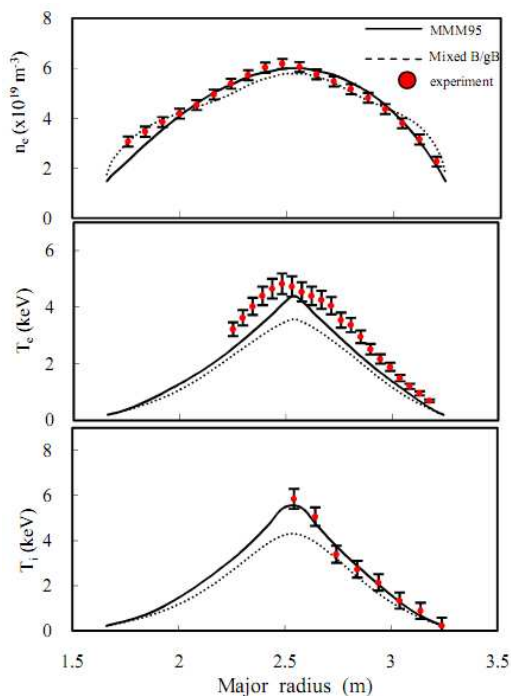
Tokamak Shot No.	DIII-D 78106 low $\rho^*$	DIII-D 78281 high $\rho^*$	DIII-D 78109 low $\rho^*$	DIII-D 78283 high $\rho^*$
$R$	1.70	1.70	1.70	1.70
$a$	0.63	0.63	0.63	0.63
$\kappa$	1.87	1.87	1.87	1.87
$B_T$	1.94	0.96	1.95	9.64
$I_p$	1.00	0.49	1.00	0.47
$n_e$	3.78	1.39	2.74	1.20
$P_{aux}$	1.50	0.38	2.00	0.51
$t_{diag}$	2.55	2.60	3.90	3.90

#### 4.1 Profile Comparison

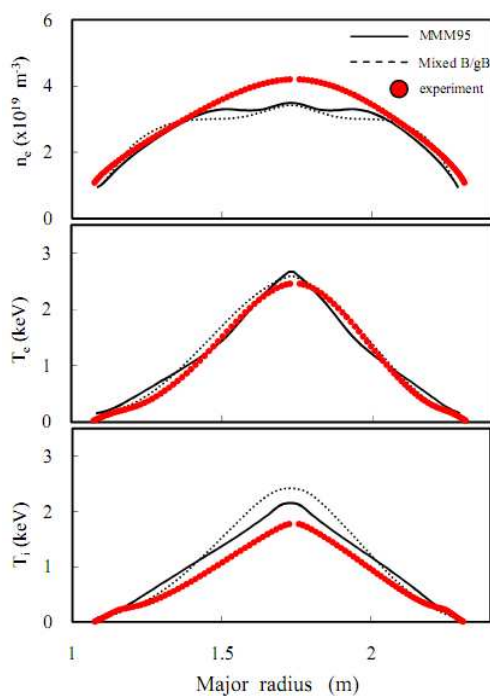
The predicted plasma profiles are carried out using either the MMM95 model or the Mixed B/gB model for 13 *L*-mode discharges from DIII-D and TFTR, including the different of systematic scans, such as gyro-radius, auxiliary heating power, plasma current and density. The details of the systematic scans are listed in Tables 2-4, including the diagnostic time. Figs.3-7 show electron density, electron temperature and ion temperature profiles from either the MMM95 model or the Mixed B/gB model for five discharges from TFTR and DIII-D. These simulation profiles are compared against experimental data. In each plot, the solid line represents the MMM95 model and the dash line represents the Mixed B/gB model. Note that the experimental data has dotted lines with error bars when it is available.

For the density profiles, each simulation result of all discharges using either the MMM95 model or the Mixed B/gB model tend to match experimental data equally well for the entire region of plasma. For the electron and ion temperature, the simulation profiles which use the MMM95 model tend to agree with the experimental data better than those using the Mixed B/gB model. It can be seen that the simulations using the Mixed B/gB model tend to under predict the experimental values.

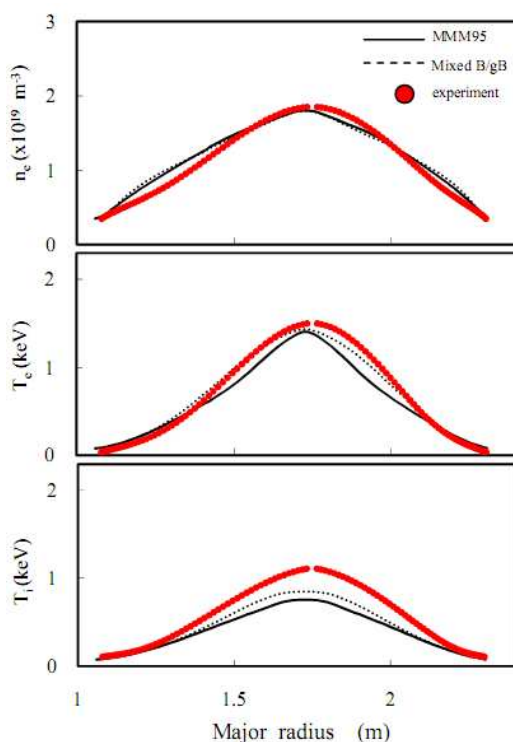

**Fig.3** The simulation profiles for TFTR 45359 discharge

**Fig.4** The simulation profiles for TFTR 45585 discharge



**Fig. 5** The simulation profiles for TFTR 50911 discharge



**Fig. 6** The simulation profiles for DIII-D 78109 discharge



**Fig. 7** The simulation profiles for DIII-D 78283 discharge

## 4.2 Statistical analysis

The statistical analysis such as the relative root mean square (RMS) deviation and the relative offset are used to quantify the comparison between the simulations and the experiments. Both are computed based on the difference between simulation profiles and experimental data. The RMS deviation of each quantity  $x$  ( $n_e$ ,  $T_e$ ,  $T_i$ ) is defined as:

$$\sigma_x = \sqrt{\frac{1}{N} \sum_{j=1}^N \left( \frac{X_j^{sim} - X_j^{exp}}{X_{max}^{exp}} \right)^2} \quad (5)$$

where  $X_j^{sim}$  and  $X_j^{exp}$  are the  $j^{\text{th}}$  data point of the simulation and experimental profiles, respectively, while  $X_{max}^{exp}$  is the maximum data point of the experimental profile of  $x$  as a function of radius which has  $N$  points in total. The RMS deviation of each discharge for any profile ( $n_e$ ,  $T_e$ ,  $T_i$ ) is designated by

$\sigma_i$ . Then the distribution of the RMS deviation over all the discharges can be characterized by the average RMS deviation as:

$$\bar{\sigma} = \frac{1}{N_s} \sum_{i=1}^{N_s} \sigma_i \quad (6)$$

and the RMS deviation is defined as:

$$\sigma_\sigma = \sqrt{\frac{1}{N_s - 1} \sum_{i=1}^{N_s} (\sigma_i - \bar{\sigma})^2} \quad (7)$$

where  $N_s$  is the number of all discharges. The relative offset of each quantity  $X$  ( $n_e$ ,  $T_e$ ,  $T_i$ ) is defined as:

$$f = \frac{1}{N} \sum_{j=1}^N \left( \frac{X_j^{sim} - X_j^{exp}}{X_{max}^{exp}} \right) \quad (8)$$

The statistical analysis is used to compare between simulation and experiment profiles. Figs. 8 – 9 show that the electron density profiles using both transport models agree with the experimental data about equally well. The RMS deviation for each discharge using the MMM95 model varies from 2.50% to 10.45% while that using the mixed B/gB model varies from 2.00% to 16.41%. For temperature profiles, the RMS deviations using the MMM95 model for the electron and ion vary from 3.34% to 21.08%, and 6.04% to 34.07%, respectively. While using the Mixed B/gB model, the RMS deviations of electron and ion temperature vary from 4.28% to 27.94%, and 4.17% to 38.87%, respectively.

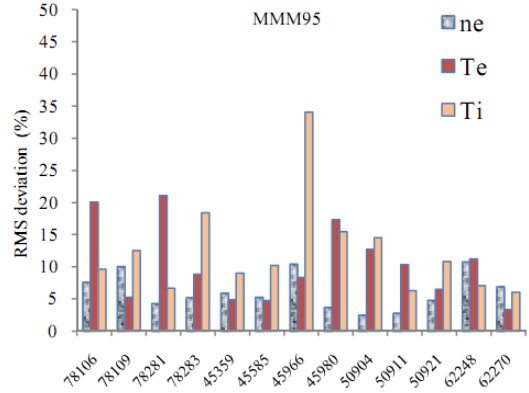


**Fig. 8** RMS deviation of simulation profiles compare with experimental data for 13 discharges from DIII-D and TFTR tokamaks using the MMM95 model.

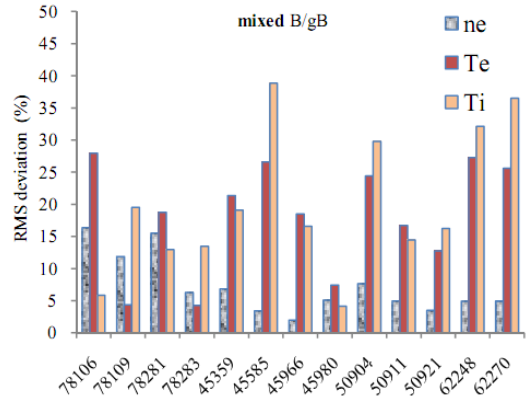


**Fig.9** RMS deviation of simulation profiles compare with experimental data for 13 discharges from DIII-D and TFTR tokamaks using the Mixed B/gB model.

The average RMS deviations ( $\bar{\sigma}$ ) and the RMS deviations of the RMS deviations ( $\sigma_\sigma$ ) for each transport model are summarized in Table 5. It can be seen that the average RMS deviations for density profile are less than 8%, and for temperature profile, are less than 20% for simulations of both transport models. It shows that the two transport models match experimental data equally well, because the difference between the average RMS deviations for each transport model and

each kind of profile is much less than the sum of them.

**Table 5** The average RMS deviations % relative to the maximum of experimental data (%).

Profile	MMM95		Mixed B/gB		$ \bar{\sigma}_{MMM95} + \bar{\sigma}_{mixed} $	$\bar{\sigma}_{MMM95} + \bar{\sigma}_{mixed}$
	$\bar{\sigma}$	$\sigma_{\sigma}$	$\bar{\sigma}$	$\sigma_{\sigma}$		
$n_e$	6.2	2.8	7.2	4.6	1.0	7.4
$T_e$	10.4	5.9	18.2	8.6	7.8	14.5
$T_i$	12.4	7.6	20.0	11.1	7.6	18.6

The simulation results of each transport model are plotted against experimental data in boundary of all discharges at the point 80% and 95% of minor radius ( $r = 0.80a$  and  $r = 0.95a$ ) are shown as Fig.10.

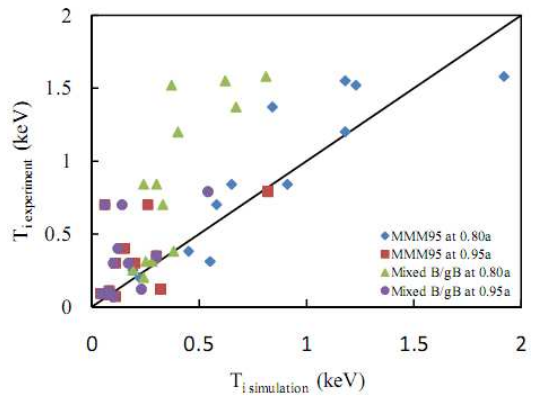
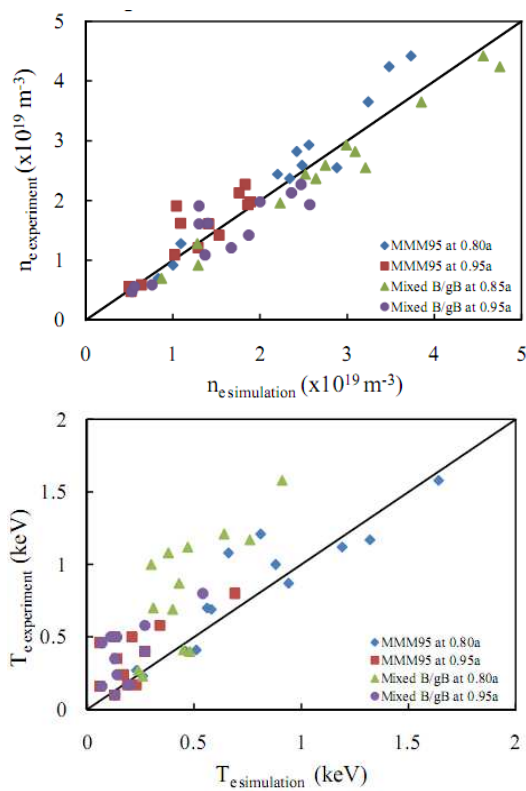


**Fig. 10** The simulation results are plotted against experimental data in boundary of all discharges at the points 80% and 95% of minor radius.

The RMS deviations for electron density, electron temperature and ion temperature discharges at the point of  $r = 0.80a$  and  $r = 0.95a$  are shown in Table 6. It can be seen that the simulation results at the inner plasma are more accurate than the edge. For comparison, the simulation profiles using the MMM95 model and the Mixed B/gB model at each point of plasma, the statistical analysis show that the MMM95 model tend to agree with experimental data more than those using the mixed B/gB model. Note that the simulations using the Mixed B/gB model tend to predict the plasma profiles that are lower than experimental data, especially electron and ion temperature profiles.

**Table 6** The RMS deviation of simulation profiles at  $r = 0.8a$  and  $r = 0.95a$  relative to the experimental data

Profile	$r = 0.8 a$		$r = 0.95a$	
	MMM95	Mixed B/gB	MMM95	Mixed B/gB
$n_e$	8.3	6.8	14.7	15.2
$T_e$	11.6	29.3	34.9	39.6
$T_i$	15.4	38.8	30.6	34.0

These RMS deviations are confirmed by the relative offset to maximum of experimental data of each transport model and each kind of profile is shown in Figs. 11-12. However, the difference between the offsets is not statistically significant. Table 7 shows that the difference between the average offset of each transport model and each kind of profile is less than the sum of the RMS deviations of the offsets.

**Table 7** The average relative offset to the maximum of experimental data (%).

Pro-file	MMM95		Mixed B/gB		$ \bar{f}_{MMM95} - \bar{f}_{mixed} $	$\bar{\sigma}_{MMM95} + \bar{\sigma}_{mixed}$
	$\bar{f}$	$\sigma_f$	$\bar{f}$	$\sigma_f$		
$n_e$	-1.2	3.4	0.8	4.8	2.0	8.2
$T_e$	-1.4	7.5	-12.5	10.2	11.2	17.7
$T_i$	1.7	10.5	-11.3	15.7	13.0	26.2

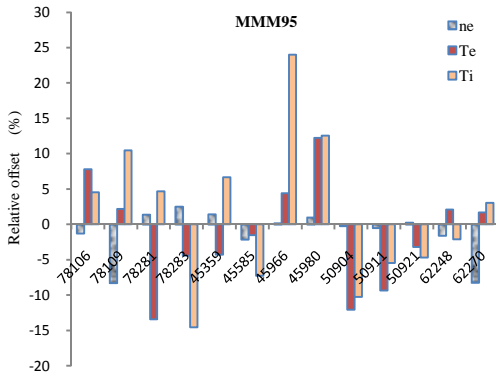


**Fig.11** Relative offset of simulation profiles compare with experimental data for 13 discharges from DIII-D and TFTR tokamaks using the MMM95 model.

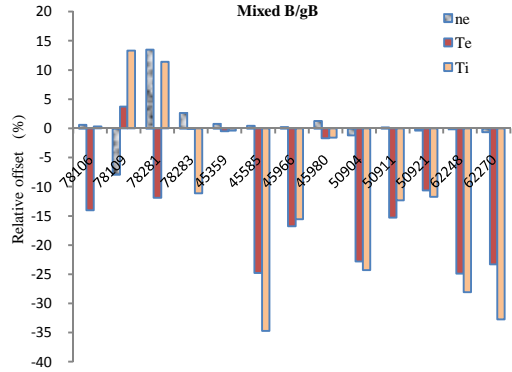


**Fig.12** Relative offset of simulation profiles compare with experimental data for 13 discharges from DIII-D and TFTR tokamaks using the Mixed B/gB model.

### 4.3 Prediction of ITER

International Thermonuclear Experimental Reactor (ITER) is a project that aims to provide understanding for controlled fusion in order to make a transition from today's studies of plasma physics to future electricity-producing fusion power plants. These developed boundary condition models are used to simulate the electron density, electron temperature and ion temperature profiles of ITER with the design parameters ( $R = 6.2$  m,  $a = 2.0$  m,  $I_p = 15$  MA,  $B_\phi = 5.3$  T,  $\kappa = 1.7$ ,  $\delta = 0.3$  and  $n_l = 1.0 \times 10^{20} \text{ m}^{-3}$ ). In these simulations we used the NBI auxiliary power 7 MW, to control the plasma heating power in L-mode, not exceeding the following empirical expression for the threshold power, taken from [13]:

$$P_{L \rightarrow H} (MW) = 2.84 M_{AMU}^{-1} B_\phi^{0.82} n_{e,20}^{-0.58} R^{1.00} a^{0.81} \quad (9)$$

The simulation results of ITER with these boundary conditions at diagnostic time 1000 seconds are shown in Fig.13. It can be seen that the simulations using MMM95 model are similar to those using Mixed B/gB model. The central and edge values of each profiles are summarized in Table 8.

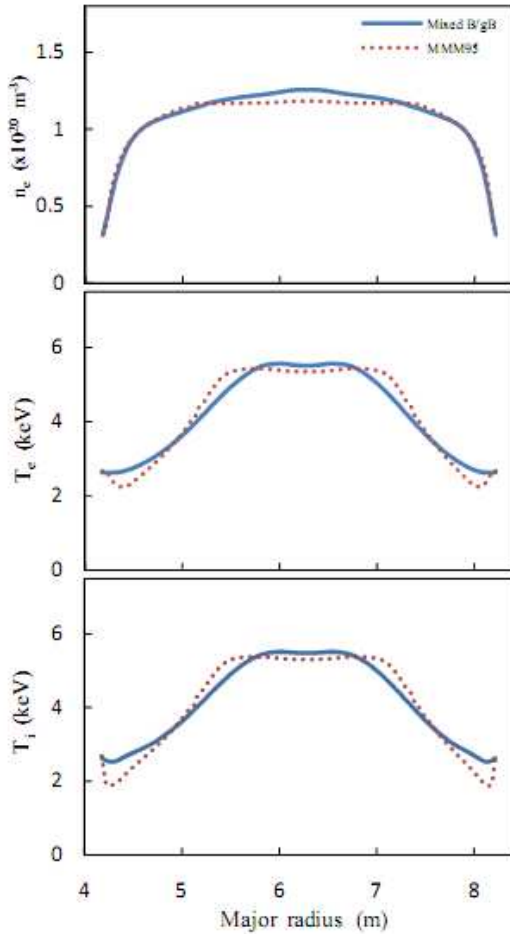


**Fig. 13** The simulation profiles of ITER in *L*-mode at diagnostic time 1000 seconds.

**Table 8** The simulation profiles at the edge and central core of plasma

Profile	Edge		Central core	
	MMM 95	Mixed B/gB	MM M95	Mixed B/gB
$n_e$ ( $\times 10^{20} \text{ m}^{-3}$ )	0.3	0.3	1.2	1.3
$T_e$ (keV)	2.7	2.6	5.4	5.6
$T_i$ (keV)	2.7	2.6	5.3	5.5

The fusion performance of ITER can be evaluated in term of Fusion  $Q$ , which can be calculated as :

$$FusionQ = \frac{5xP_{\alpha,ave}}{P_{aux}} \quad (10)$$

where  $P_{\alpha,ave}$  is an average alpha power and  $P_{aux}$  is an auxiliary heating power (7 MW in these simulations). The alpha power production of ITER from both of the Mixed B/gB model and the MMM95 model are plotted as a function of time. They are shown in Fig.14.

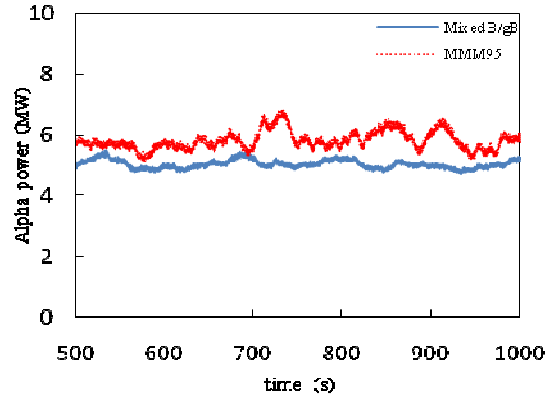


**Fig. 14** The alpha power production from the Mixed B/gB model and the MMM95 model are plotted as a function of time.

It can be seen that the alpha power production from the simulation with the MMM95 model is slightly higher than that from the simulation with the Mixed B/gB model. The average alpha power are 5.80 MW and 5.02 MW for the simulations using MMM95 model and Mixed B/gB model, respectively. This is not surprising since the temperature and density profiles for both simulations are quite similar. Therefore, the Fusion  $Q$  in *L*-mode of ITER from the simulations with the MMM95 model and the Mixed B/gB model are predicted to be 4.12 and 3.59, respectively. These Fusion  $Q$  are compared with the *H*-mode simulations from Ref.[13] and Ref.[14], which have three pedestal width models considered: magnetic and flow shear stabilization ( $\Delta\alpha ps^2$ ), flow shear stabilization ( $\Delta\alpha\sqrt{pRq}$ ) and normalized poloidal pres-

sure  $(\Delta\alpha R\sqrt{\beta_{\theta,ped}})$ . The comparison of these Fusion Q are shown in Table 9.

**Table 9** The comparison of Fusion Q between *L*-mode and *H*-mode with three pedestal width models.

transport model	<i>L</i> -mode	$\Delta\alpha ps^2$		$\Delta\alpha\sqrt{pRq}$		$\Delta\alpha R\sqrt{\beta_{\theta,ped}}$	
		Ref [13]	Ref [14]	Ref [13]	Ref [14]	Ref [13]	Ref [14]
Mixed B/gB	3.59	1.7	3.4	1.5	3.0	2.0	4.1
MMM95	4.12	6.2	-	5.9	-	6.4	-

It can be seen that the ITER performances in *L*-mode and *H*-mode are quite similar. This is not surprising since the boundary in *L*-mode and *H*-mode are not much different.

## 5. Conclusion

The models for predicting temperature and density boundary conditions are developed using an empirical approach by optimizing against the experimental data obtained from the latest public version of the International Pedestal Database (version 3.2). The RMSEs of temperature and density at the boundary of the *L*-mode plasma are found to be 24.41% and 14.27%, respectively. Self-consistent simulations of *L*-mode plasma in DIII-D and TFTR tokamaks are carried out using 1.5D integrated predictive modeling code, BALDUR. The combination of anomalous transport models either the MMM95 model or the Mixed B/gB model, together with the developed boundary condition models, are used to simulate the time evolution of electron density, electron and ion temperature profiles for 13 *L*-mode discharges from DIII-D(4) and TFTR(9) tokamaks. It is found that the simulation results from both transport models match experimental data

equally well. The statistical analysis is carried out and it is found that the average relative root mean square (RMS) deviation for each model and each kind of profile is less than the scatter within each transport model from one discharge to another. The RMS deviation of all discharges from either the MMM95 model or the Mixed B/gB model for electron density varies from 2.00% to 16.41%, while electron temperature varies from 3.34% to 27.94%, and ion temperature varies from 4.17% to 38.87%. The average relative offset from the MMM95 model for electron density, electron temperature and ion temperature are -1.19%, -1.38% and 1.65%, while from the Mixed B/gB model are 0.77%, -12.54% and -11.35%, respectively.

These boundary conditions are used to simulate the plasma profiles in *L*-mode of ITER. The simulations using the MMM95 model and the Mixed B/gB model are very similar. For the fusion performance in *L*-mode of ITER, the Fusion Q from the simulations are predicted to be 4.12 for the MMM95 model and 3.59 for the Mixed B/gB model. Table 9 shows that the Fusion Q in *L*-mode simulation using the Mixed B/gB model is higher than that in Ref.[14] but similar to that in Ref.[14], while the MMM95 model gives a lower fusion Q than that in Ref.[14].

## 6. Acknowledgments

This work is supported by Faculty of Applied Science, King Mongkut's University of Technology North Bangkok and by Commission on Higher Education (CHE) and the Thailand Research Fund (TRF) under Contract No. RMU5180017, and the Thailand National Research University Project.

## 7. References

- [1] J. Wesson, *TOKAMAK*, 3th Edition, Oxford, 2004.
- [2] R. Aymar *et al.*, Plasma Phys. Control. Fusion, Vol. 44, p. 519, 2002.
- [3] G. Bateman *et. al.*, Phys. Plasmas, Vol. 5, p. 1793, 1998.
- [4] T. Onjun *et. al.*, Phys. Plasmas, Vol. 8, p. 975, 2001.
- [5] A. Siriwitpreecha *et al.*, Proceeding of 11th Nuclear and Science Technology Conference, Bangkok, Thailand, 2-3 July 2009. PS14
- [6] C. E. Singer *et al.*, Comput. Phys. Commun, Vol. 49, pp. 399, 1988.
- [7] D. Hannum *et al.*, Phys. Plasmas, Vol. 8, p. 964, 2001.
- [8] T. Onjun *et al.*, Phys. Plasmas, Vol. 8, p. 975, 2001.
- [9] M. Erba *et al.*, Plasma Phys. Control. Fusion Vol. 39, p. 261, 1997.
- [10] Linda E. Sugiyama, *L-mode Confinement Predictions for Burning Plasma Experiments*, MIT, USA., December 4, 2002.
- [11] R. Hiwatari *et al*, *Transport Simulation of JT-60U L-mode dis-charges*, Journal of the Physical Society of Japan, Vol. 67, pp. 147-157, 1998.
- [12] K. S. Riedel, *On dimensionally correct power law scaling expressions for L-mode confinement*, Courant Institute of Mathematical Sciences, New York U., 1-27.
- [13] Shimomura Y. *et.al* 2000 *Proc. 18<sup>th</sup> IAEA Conf.* (Sorrento, Italy)
- [14] T. Onjun *et al.*, Journal of Physics: Conference Series, Vol.123, 012034, 2008.
- [15] T. Onjun and Y. Pianroj, Nucl. Fusion, Vol. 49, p. 075003, 2009.